AIAA JOURNAL
Vol. 35, No. 1, January 1997

Low Flow-Noise Microphone for Active Noise Control Applications

R. S. McGuinn,* G. C. Lauchle,† and D. C. Swanson‡
Pennsylvania State University, University Park, Pennsylvania 16802

A method that couples output from a hot-wire anemometer with that of a microphone to reduce flow-induced pseudonoise from the microphone signal was developed. In these experiments, a microphone and a hot-wire sensor were placed in a well-defined low-speed turbulent flow in a rectangular duct. Controlled acoustic noise, both random and time harmonic, was superimposed on the flow noise by placing a speaker source close to the entrance of the duct. Detailed studies of the coherence between the hot-wire and microphone signals in the presence of flow and acoustic noise indicated that the proper combination of the two signals could reduce the turbulence noise contamination in the microphone signal. Subsequent tests demonstrated that using an adaptive least-mean-square algorithm to filter the hot-wire signal before subtracting it from the microphone signal produced broadband flow noise attenuation on the order of 20 dB at frequencies below 100 Hz and spectra that approached those of the uncontaminated microphone signal. Moreover, the resulting "hot-mic" signal retains the acoustic pressure of interest, making it an ideal sensor for use in active noise control applications where the sensing or error microphone must be placed in a flowfield.

Nomenclature

c	= filtered hot-wire signal
d_h	= hydraulic diameter
$E\{\}$	= expectation operator
er	= error signal
f	= frequency, Hz
$G_{xx}(f)$	= autospectral density estimate
H	= Fourier transform of h
h	= filter impulse response
M	= Fourier transform of m
m	= microphone signal
N	= number of filter coefficients
n_d	= number of ensemble averages
p	= pressure
u	= velocity
W	= Fourier transform of w
w	= hot-wire signal
x	= spatial direction
γ^2	= ordinary coherence function
ε_r	= random error
μ	= convergence coefficient, fluid viscosity
ρ	= fluid density

Introduction

MANY active noise control problems involve placing a sensing microphone, error microphone, or both in a flow. One such example is the active control of fan noise in an air conditioning duct. A microphone placed in a flow senses aerodynamic pressure fluctuations (pseudonoise) as well as acoustic pressure fluctuations. Because the microphone senses these fluctuations simultaneously, the active control system will try to cancel the flow-induced noise as well as the actual noise. However, the directly radiated noise due to turbulent pressure fluctuations is much smaller than the pseudonoise imposed by them on a microphone, and the phase speeds of the two different types of pressure fluctuations are also considerably different. As a result, active cancellation of the flow noise is not accomplished. Instead, the level of the pseudo-pressure fluctuations imposes a limit below which active acoustic attenuation cannot be achieved.[1–3] Consequently, removing the flow noise from the microphone signal, with minimal loss of amplitude or phase information of the acoustic noise, is important for active noise control applications.

Methods for eliminating flow noise from a microphone signal include placement of an open-cell foam ball or a streamlined nose cone over the microphone diaphragm, incorporation of a bias error correction in the estimate of the pressure spectrum,[4] or spatial averaging using data processing techniques such as the cross spectral density, correlation function, coherence function, or transfer function between two or more microphones spaced beyond the turbulence correlation length.[5–8] The drawbacks of the preceding methods include, respectively, too much flow blockage, loss of phase information of the pressure, or too little turbulence suppression. These issues make them undesirable or useless for active noise control applications. Methods that do not result in loss of the pressure data include the use of transducers large enough to average out the turbulent fluctuations,[9] transducer arrays,[10] and sampling or slit tubes.[11–15] These techniques may result, however, in undesirable pressure attenuation, additional expense, or increased length (volume) requirements. Using a slit tube in conjunction with the microphone, a means of turbulence noise suppression currently used in some active noise control applications provides little or no flow noise attenuation for frequencies less than 70 Hz (Ref. 16) and requires a longer sensing length than typically desired.

Objective

The objective of this research is to remove flow noise from the microphone signal with minimal loss of phase or amplitude of the acoustic pressure signal of interest while maintaining minimum impact on sensor space requirements. In particular, the emphasis for flow noise reduction is placed on the frequency range $f < 100$ Hz. In this investigation flow noise attenuation is performed by combining the response of the microphone with a signal from a hot-wire sensor placed in the same flow. Although the purpose of this research is to devise a low flow-noise microphone that functions well under the restrictive requirements of the active noise control application, active noise control, per se, is not discussed in detail. In addition, no attempt is made to optimize the adaptive algorithms.

Received March 15, 1996; presented as Paper 96-1784 at the AIAA/CEAS 2nd Joint Aeroacoustics Conference, State College, PA, May 6–8, 1996; revision received Sept. 9, 1996; accepted for publication Sept. 20, 1996; also published in *AIAA Journal on Disc*, Volume 2, Number 2.

*Graduate Student, Department of Aerospace Engineering. Student Member AIAA.

†Professor of Acoustics, Graduate Program in Acoustics and Applied Research Laboratory. Member AIAA.

‡Professor of Acoustics, Graduate Program in Acoustics and Applied Research Laboratory.

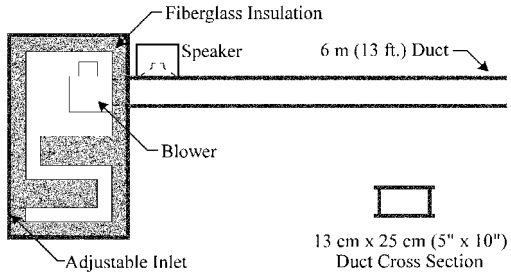

Fig. 1 Rectangular duct test facility.

Experimental Setup

Experiments were performed in a 0.25 × 0.13 × 4 m (0.8 × 0.4 × 13 ft) rectangular duct, illustrated in Fig. 1, with airflow provided by a variable speed centrifugal blower. A hot-wire probe and a microphone were mounted on a support stand on the centerline at the exit of the duct where the flow conditions, mean velocity equal to 7 m/s (23 ft/s) and turbulence intensity of 10%, approximated those expected in a typical active noise control application. A signal generator provided a random or time-harmonic output that was amplified and used to drive a speaker mounted in the top section of the duct near the exit of the blower.

A single-sensor hot-wire probe 0.005 mm (0.0002 in.) in diameter with a sensing length of 1.5 mm (0.06 in.) was used to measure velocity. Acoustic measurements were obtained with a pinhole microphone[17] consisting of a 12.7-mm (1/2-in.) free-field condenser microphone with a streamlined 0.8-mm (1/32-in.) inner diameter pinhole/tube nose cone instead of the standard protective grid. The pinhole nose cone provided a more streamlined surface than the standard protective grid and also greatly reduced the sensing area to better approximate a "point" measurement. The resonance frequency of the pinhole cavity was approximately 1200 Hz, above the frequencies of interest in this study.

Data were acquired using a fast Fourier transform analyzer and simultaneous time capture to a computer hard drive at a sampling rate of 2048 samples/s. Spectral analysis employed antialias filtering and a Hanning window. There is no bias error from spectra to spectra because the sampling rate and analysis bandwidth (2 Hz) remained the same for all samples. The random error, also the same for all cases, can be computed from[18]

$$\varepsilon_r[\hat{G}_{xx}(f)] = 1/\sqrt{n_d} \tag{1}$$

where the number of ensemble averages $n_d = 100$. Both the hot-wire and microphone spectral data were repeatable to within 1 dB for each condition tested, which is consistent with the estimated random error of 10%.

Results and Discussion

Coherence

The pressure–velocity relationship for low-speed incompressible flow can be derived by combining the divergence of the momentum equation with the continuity equation to yield Poisson's equation,[19]

$$\nabla^2 p = -\rho \frac{\partial^2 (u_i u_j)}{\partial x_i \partial x_j} \tag{2}$$

Solution of Eq. (2) reveals that pressure fluctuations at a given point result from an integration of weighted velocity fluctuations over all space.

A hot-wire sensor provides a measure of velocity fluctuations but it does so over only a small and finite length. In addition, a hot-wire signal is proportional to the square root of velocity.[20] For the low-speed, incompressible flow of interest here, we know from Euler's equation that velocity is proportional to the square root of pressure. The output from a hot-wire anemometer is therefore a nonlinear representation of the fourth root of the local aerodynamic pressure fluctuations. A microphone, on the other hand, provides a direct and linear measure of pressure.

To determine the feasibility of using a hot wire to provide an aerodynamic pressure signal that can be combined with a microphone signal, coherence measurements between the hot-wire signal and a signal from a nearby microphone placed in the same flowfield have been carefully examined. The ordinary coherence function between the hot-wire signal $w(t)$ and the microphone signal $m(t)$ is defined as[18]

$$\gamma^2_{wm}(f) = \frac{|G_{wm}(f)|^2}{G_{ww}(f)\, G_{mm}(f)}, \qquad 0 \leq \gamma^2_{wm}(f) \leq 1 \tag{3}$$

A high coherence, $\gamma^2_{wm}(f)$ near 1, between the two signals in the presence of flow implies that both sensors are responding to similar fluid dynamic fluctuations. In such a case, properly combining the hot-wire signal with the microphone signal may lead to a reduction in the flow noise response of the microphone.

A systematic study was performed to determine the optimum configuration of the hot-wire sensor and microphone to promote high coherence between them. We know from Eq. (2) that the fluctuating pressure at a point is the result of the integrated velocity fluctuations over a much larger volume. To reduce the measurement area of the microphone and thereby reduce the area of contributing velocity fluctuations, the standard protective grid of the microphone was replaced with a pinhole nose cone as shown in Fig. 2. The pinhole diameter was 0.8 mm (1/32 in., $d = 0.005 d_h$), and the tube was 2.54 cm (1 in., $l = 0.15 d_h$) long. The pinhole microphone[17] exhibits a slight attenuation ($\sim$1 dB) of the pressure but still maintains a flat frequency response except at the cavity resonance frequency. For the pinhole size used here, a comparison calibration showed the resonance frequency to be at approximately 1200 Hz, which is above the frequencies of interest in this study and does not adversely affect the pressure measurements.

Variations in the placement of the pinhole microphone and the hot-wire sensor relative to the pinhole opening were tested. It was found that the highest coherence between the hot wire and microphone occurred when the pinhole microphone was aligned with the flow with the pinhole pointing in the upstream direction as shown in Fig. 2. In this manner, it will behave like a total head probe. The microphone vent removes the effect of the mean pressure, and the resulting pressure signal is representative of fluctuating pressures traveling in the freestream direction. It therefore responds more to streamwise velocity fluctuations and mean shear rather than normal velocity shear that is dominant when the microphone is mounted flush with the duct wall, normal to the flow. When the microphone is oriented in the streamwise direction, broadband flow noise measured by the microphone is approximately 5 dB higher than that measured with the microphone normal to the flow but in the same location. The objective of the research, on the other hand, is to reduce the flow noise inherent in the microphone signal. This increase in flow noise is an issue to be concerned with and is discussed in more detail later.

The hot-wire placement was determined after tests that included streamwise and spanwise orientation (both of which, by virtue of the fact that a single sensor was used, contain transverse velocities) as well as variations in location with respect to the pinhole opening. Highest coherence levels were obtained with the hot-wire sensor placed upstream of the centerline of the pinhole and oriented to measure the streamwise velocity component. The optimum configuration is shown in Fig. 2, where the hot-wire sensor is located 0.5 mm (0.02 in.) upstream of the center of the pinhole opening. This configuration is used for all measurements reported herein.

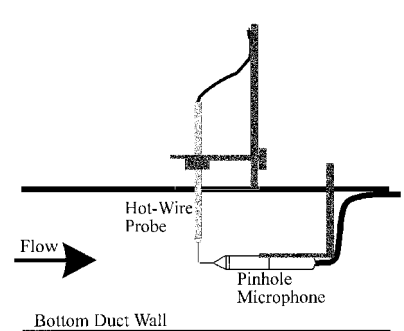

Fig. 2 Hot-wire and microphone placement in duct.

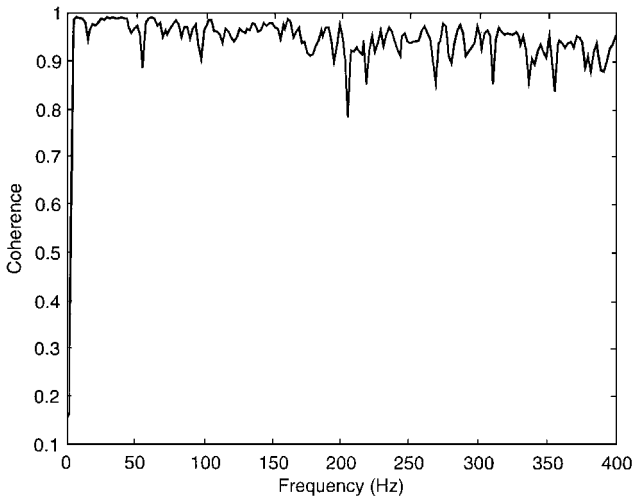

Fig. 3 Measured coherence function between hot-wire sensor and microphone in flow only.

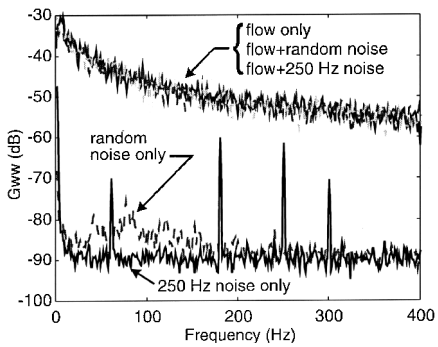

Fig. 4 Hot-wire autospectral densities.

Measurements were made to ensure that placing the hot wire just upstream of the pinhole opening of the microphone did not alter the microphone response. A comparison of the microphone response with and without the hot wire in front of the opening revealed that, for the frequency range of interest, the interference is negligible. It is expected that the hot wire does affect the microphone response at higher frequencies (the hot-wire vortex shedding frequency $\sim$305 kHz based on a Strouhal number of 0.2 for cylinder vortex shedding).

The measured coherence function between the hot-wire and microphone signals when placed in the flow in the duct is shown in Fig. 3. The coherence levels are high, greater than 0.9 over the entire frequency range and approaching unity at frequencies below 100 Hz. These high levels indicate that combination of the two signals for removal of flow noise from the pressure signal is feasible.

Detailed studies of autospectral density of each sensor and the measured coherence function between them were performed with the sensors in the presence of both aerodynamic and acoustic excitation. Random and time-harmonic acoustic noise was introduced into the duct by the speaker located near the entrance of the duct (Fig. 1). The speaker output was adjusted so that the overall acoustic sound pressure level at the microphone in the duct without flow matched the overall sound pressure level perceived by the microphone placed in the same location in the duct with flow only (approximately 80 dB re: 20 μPa). The sinusoidal acoustic noise was generated by driving the speaker at 250 Hz. This frequency was chosen by virtue of the fact that it is below the plane wave cutoff frequency of the duct and therefore should be a plane wave disturbance. (The cut-on frequency of the first duct cross mode is approximately 650 Hz.) Furthermore, 250 Hz is not a harmonic of 60 Hz line noise.

The autospectral densities of the hot-wire and microphone responses are plotted in Figs. 4 and 5, respectively. In these and all subsequent plots, the dB scale is referenced to 1 V. The five curves in each plot represent each of the five test cases considered: flow

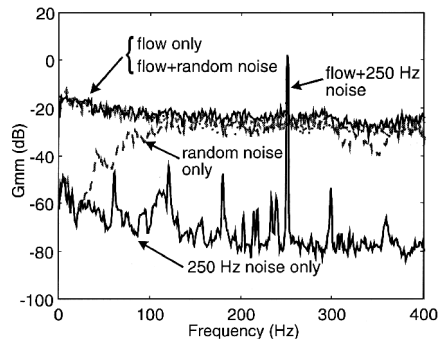

Fig. 5 Microphone autospectral densities.

only, flow + random acoustic noise (white noise), flow + 250 Hz time-harmonic acoustic noise, random noise only, and 250 Hz sine wave noise only. Reflections from the duct walls and higher-order duct modes are present but do not affect the intent or results of this study and, therefore, will not be discussed. Note that, although both the microphone and the hot-wire sensor were calibrated prior to the experiments, no calibrations were applied to the output from either sensor during these tests. This is because we are only interested in relative changes in the microphone signal due to the signal conditioning using the hot wire and least-mean-square (LMS) algorithm. Coherence functions never require calibrated signals because the calibration constant cancels in its definition [Eq. (3)]. Additionally, the raw voltages are important in the signal conditioning since it is these signals that are to be combined. The coherence measurements will therefore indicate whether the uncalibrated, nonlinear hot-wire signal, proportional to the fourth root of pressure, may be combined with a microphone signal, linearly proportional to the pressure, to remove the flow-induced noise.

In Fig. 4, it is clear from the collapse of the data for the first three cases that the hot-wire response is aerodynamically dominated in the presence of flow regardless of the speaker-generated noise. This effect is expected since the level of the acoustic noise, adjusted to give the same overall sound pressure level at the microphone as the flow-induced noise, produces fluctuating velocities that are much smaller (on the order of 50 times smaller) than those generated by the flow. It can also be seen by the spectrum levels that most of the flow energy is contained at the lower frequencies. In the absence of flow, the hot-wire response tends to be buried in the anemometry system noise.

The microphone responses plotted in Fig. 5 show that the microphone signal is highly contaminated by flow noise especially at frequencies below 100 Hz. The shape of the spectra for the cases in the presence of flow are almost identical to each other and to those of the hot-wire spectra for the same conditions (the plot scales are different). The addition of flow to the random noise does not significantly alter the spectrum from the random-noise-only spectrum above 100 Hz but causes a large increase in level below 100 Hz where most of the flow contamination is concentrated. A broadband increase of nearly 50 dB results from adding flow to the 250 Hz noise.

The data presented in Figs. 4 and 5 clearly illustrate the need for flow noise suppression for the microphone response, especially for frequencies below 100 Hz. The data also show that the hot wire does respond to acoustic excitation, but in the presence of flow the acoustic response is masked by the response to the aerodynamic effects.

To determine whether the signals from the two sensors may be combined to reduce flow noise, coherence function measurements between the hot-wire and microphone signals were studied for the same flow and acoustic conditions. The measured coherence function for the sensors placed in the duct with flow only was given in Fig. 3. Similar plots of the measured coherence functions for the other four cases are given in Figs. 6–9.

The coherence functions are almost identical for the cases with flow only (Fig. 3) and flow + 250 Hz acoustic noise (Fig. 6) with the exception of a decrease at 250 Hz. The similarity was expected since the hot-wire and microphone spectra for these conditions, too, were nearly identical. The drop in coherence at 250 Hz is due to the fact that the microphone response to the tone is strong but the

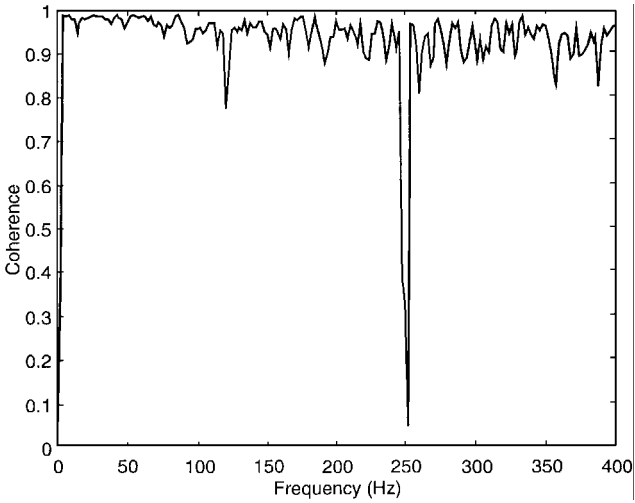

Fig. 6 Measured coherence function for flow + 250 Hz case.

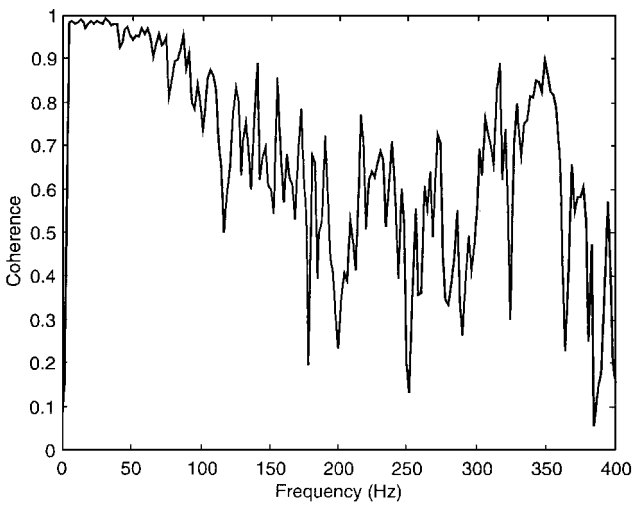

Fig. 7 Measured coherence function for flow + random noise case.

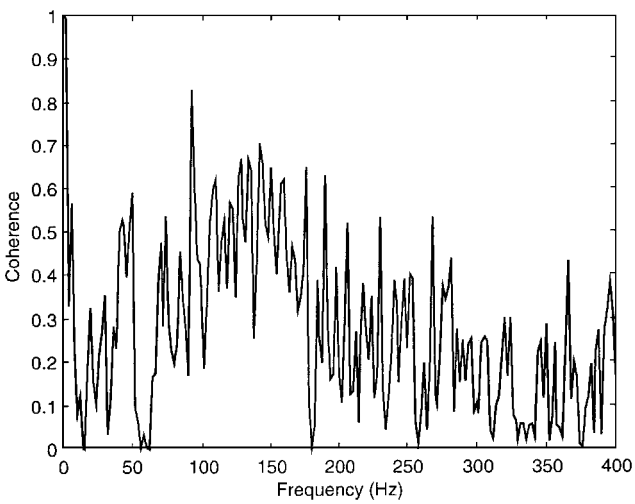

Fig. 8 Measured coherence function for random noise only case.

hot-wire response is still dominated by the aerodynamic velocities rather than the acoustic velocity fluctuations associated with the tone. The coherence measured with both flow and random noise (Fig. 7) is high for frequencies less than 100 Hz because most flow noise contamination occurs in this range, but drops off at higher frequencies. When only acoustic excitation is present (Figs. 8 and 9) the coherence levels are much lower than in the presence of flow with the exception of the 250 Hz tone.

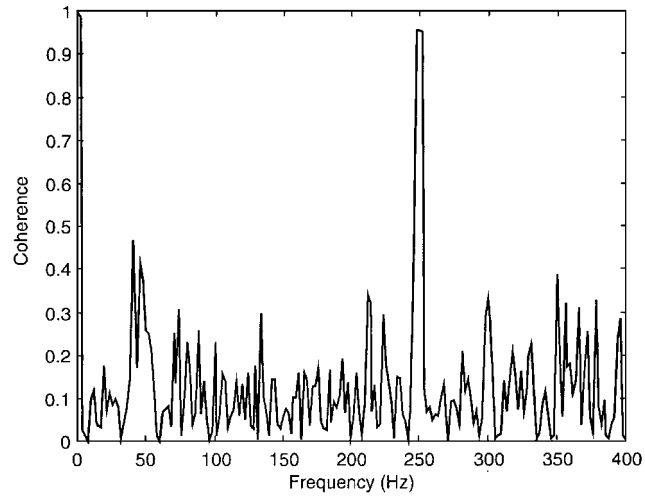

Fig. 9 Measured coherence function for 250 Hz only case.

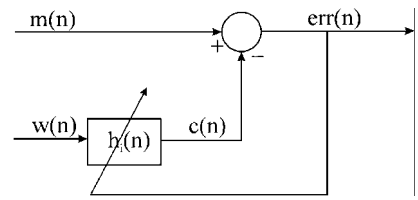

Fig. 10 Schematic representation of the hot mic.

Note that the coherence levels are generally high in the presence of flow, especially where desired at frequencies below 100 Hz, and that the levels are significantly lower in the absence of flow. This effect is desirable because we want to combine the signals to remove the effects of flow (pseudonoise) from the microphone signal but leave the acoustic pressure signal (in this case, the random or 250 Hz noise) unaltered. Since the fluid dynamic response of the two sensors is coherent but the acoustic response is not, a proper combination of the two signals should result in attenuation or elimination of the (coherent) fluid dynamic contribution from the signals.

Flow Noise Reduction

Flow noise reduction was achieved by adaptively filtering the hot-wire signal and then subtracting it from the microphone signal. This combination was performed with the 10 second time-capture data using an LMS algorithm, and for the sake of brevity, the filtered hot-wire/microphone signal combination, which performs as a single sensor, will be referred to as a "hot mic." The schematic for the hot-mic is given in Fig. 10. No attempt has been made to optimize the adaptive algorithm or the convergence speed, and as in the coherence measurements, no calibration is applied to either the hot-wire or microphone signal.

In this algorithm, the digitized hot-wire signal $w(n)$ is passed through the adaptive filter $h_i(n)$ and then subtracted from the microphone signal $m(n)$ to produce an error signal $\mathrm{err}(n)$. The output of the filter $c(n)$ should be that part of the hot-wire signal that is coherent with the microphone signal, i.e., the noise caused by turbulence pressure fluctuations. The subtraction of $c(n)$ from $m(n)$ will then produce an output proportional to the acoustic pressure fluctuations with the pseudonoise component removed.

The i-filter coefficients were updated using an LMS algorithm,

$$h_i(n+1) = h_i(n) + 2\mu w(n)\mathrm{err}(n) \tag{4}$$

In all cases, the convergence coefficient was set at $\frac{1}{10}$ of its maximum value, $\mu_{\max}$, which was determined from the following stability criterion:

$$\mu_{\max} \quad \frac{1}{N \cdot E\{w^2(n)\}} \tag{5}$$

The filter coefficients were initially set according to

$$H(f) = M(f)/W(f) \tag{6}$$

where $M(f)$ and $W(f)$ are the Fourier transforms of the microphone and hot-wire responses, respectively. The impulse response was then obtained by taking the inverse Fourier transform of $H(f)$ and truncating it to the desired number of filter coefficients. The number of points used for the Fourier transforms was varied, and, as expected, the greater the number of points, the better the filter approximated the optimal transfer function between the hot-wire sensor and microphone. For the sake of brevity, however, variations in the n-point Fourier transforms will not be discussed further. Only those performed with 1024 points are included in this paper.

In the hot-mic algorithm, the first 1024 points of the hot-wire and microphone data records were used to calculate the initial filter coefficients as discussed earlier. The remaining data points were then treated as real-time data to which the algorithm adapted. After the 10-s sample was processed, the hot-mic output (the error signal), which ideally contains acoustic pressure information with the flow-induced pseudonoise removed, was compared with the microphone spectra with and without flow contamination. Figure 11 is a plot of this comparison for the case of random noise. In this plot, the solid line represents the spectrum of the hot-mic signal, the dashed line represents the microphone signal in the presence of random noise without flow contamination, and the dotted line shows the microphone response to the random noise in the presence of flow.

The desired result is for the spectrum of the hot-mic signal to approach that of the microphone signal in the absence of flow. It can be seen from Fig. 11 that the hot-mic signal does indeed approach that of the uncontaminated microphone signal, resulting in a flow noise attenuation of greater than 15 dB at below 100 Hz and better spectral approximation to the uncontaminated microphone signal out to 400 Hz.

By increasing the number of filter coefficients, the approximation of the error signal to the uncontaminated microphone increases. Figure 12 shows the same spectral comparison with 16 filter coefficients. Flow noise attenuation is increased an additional 5–10 dB at frequencies below 100 Hz without losing the pressure information at the higher frequencies. A point will be reached, in this case with approximately 100 filter coefficients, where the slow convergence of the LMS algorithm cannot keep up with the coefficient update, especially since the coherence between the hot-wire and microphone signals decreases as frequency increases. The important result, however, is that flow noise attenuation in the pressure signal of 20 dB or more and a better spectral approximation to the uncontaminated pressure signal is possible with very few filter coefficients and a simple LMS adaptive algorithm. Moreover, the flow noise reduction is sufficient to overcome the increase caused by streamwise orientation of the microphone.

The same type of comparison was also made with the 250 Hz noise superimposed on the flow. Figures 13 and 14 illustrate how low-frequency as well as higher-frequency turbulence suppression was attained with just 4 and 16 filter coefficients, respectively. Moreover,

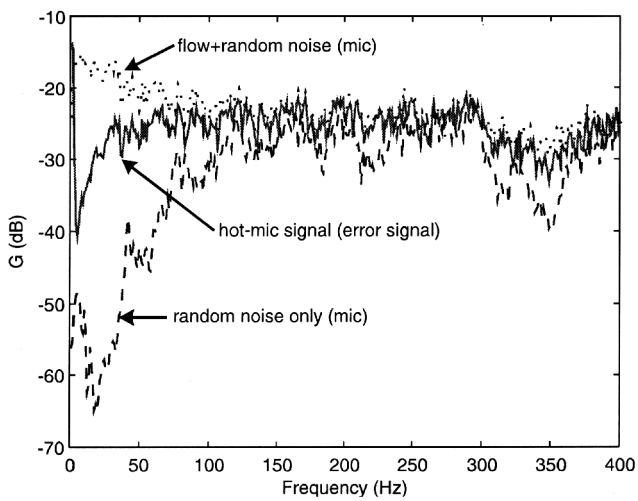

Fig. 11 Autospectral densities of microphone and error signals, random noise, four coefficients, $\mu = 0.1$.

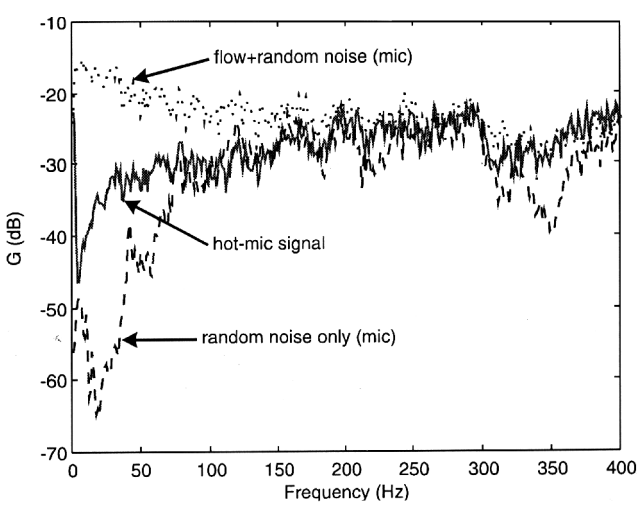

Fig. 12 Autospectral densities of microphone and error signals, random noise, 16 coefficients, $\mu = 0.025$.

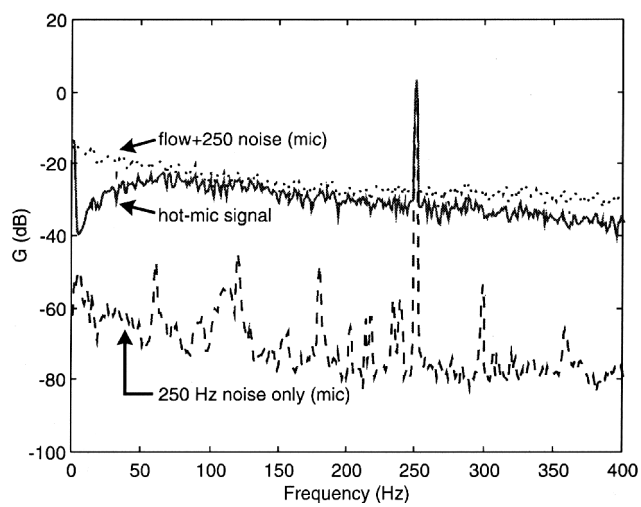

Fig. 13 Autospectral densities of microphone and error signals, 250 Hz noise, four coefficients, $\mu = 0.1$.

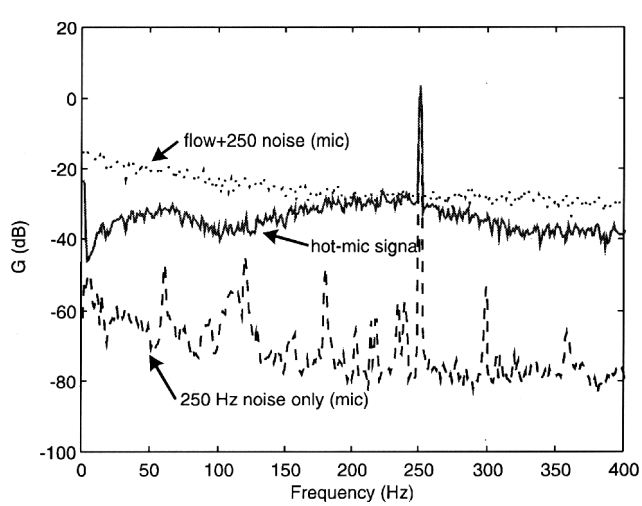

Fig. 14 Autospectral densities of microphone and error signals, 250 Hz noise, 16 coefficients, $\mu = 0.025$.

the flow noise suppression was performed without reducing the level of the acoustic pressure fluctuations at 250 Hz.

Conclusions

A hot-wire and a microphone signal may be combined to suppress turbulence-induced pseudonoise from the microphone signal without losing the acoustic pressure signal. Measured coherence levels between a raw hot-wire signal and the signal from a pinhole microphone located 0.5 mm downstream of the hot-wire sensor were high over a wide frequency range in the presence of flow but low in the absence of flow, indicating that the two signals could be combined to remove the coherent (flow-induced) part. Adaptively filtering the hot-wire signal using an LMS algorithm before subtracting it from the flow-contaminated microphone signal results in the hot-mic output that more closely resembles that of the uncontaminated microphone signal. Flow noise suppression on the order of 20 dB is attained at frequencies below 100 Hz. In addition, attenuations of more than 10 dB may be observed at higher frequencies. Furthermore, the resulting hot-mic signal retains the acoustic pressure information of interest, making the hot-mic an ideal sensor for use in active noise control applications where the sensing or error microphone must be placed in a flowfield.

Acknowledgments

The authors would like to acknowledge Bill Patrick and the United Technologies Research Center for the sponsorship of this work.

References

[1]LaFontaine, R. F., and Shepherd, I. C., "An Experimental Study of a Broadband Active Attenuator for Cancellation of Random Noise in Ducts," *Journal of Sound and Vibration*, Vol. 91, No. 3, 1983, pp. 351–362.

[2]Nakamura, A., Sugiyama, A., Tanaka, T., and Matsumoto, R., "Experimental Investigation for Detection of Sound-Pressure Level by a Microphone in an Airstream," *Journal of the Acoustical Society of America*, Vol. 50, No. 1, 1971, pp. 40–46.

[3]Shepherd, I. C., LaFontaine, R. F., and Cabelli, A., "Active Attenuation in Turbulent Flow Ducts," *Proceedings of Inter-Noise 84 Conference* (Honolulu, HI), Noise Control Foundation, New York, 1984, pp. 497–502.

[4]Lauchle, G. C., "Effect of Turbulent Boundary Layer Flow on Measurement of Acoustic Pressure and Intensity," *Noise Control Engineering Journal*, Vol. 23, No. 2, 1984, pp. 52–59.

[5]Munro, K. H., and Ingard, U. K., "On Acoustic Intensity Measurements in the Presence of Mean Flow," *Journal of the Acoustical Society of America*, Vol. 65, No. 6, 1979, pp. 1402–1409.

[6]Chung, J. Y., "Rejection of Flow Noise Using a Coherence Function Method," *Journal of the Acoustical Society of America*, Vol. 62, No. 2, 1977, pp. 388–395.

[7]Alfredson, R. J., and Loh, M., "The Multiple Coherence Method for Reducing Flow Noise on Microphones," *Proceedings of Inter-Noise 91 Conference*, Australian Acoustical Society, Sydney, Australia, 1991, pp. 1117–1120.

[8]Chung, J. Y., and Blaser, D. A., "Transfer Function Method of Measuring Acoustic Intensity in a Duct System with Flow," *Journal of the Acoustical Society of America*, Vol. 68, No. 6, 1980, pp. 1570–1577.

[9]Corcos, G. M., "Resolution of Pressure in Turbulence," *Journal of the Acoustical Society of America*, Vol. 35, No. 2, 1963, pp. 192–199.

[10]Shepherd, I. C., LaFontaine, R. F., and Cabelli, A., "The Influence of Turbulent Pressure Fluctuations on an Active Attenuator in a Flow Duct," *Journal of Sound and Vibration*, Vol. 130, No. 1, 1989, pp. 125–135.

[11]Nakamura, A., Matsumoto, R., Sugiyama, A., and Tanaka, T., "Some Investigations on Output Level of Microphones in Air Streams," *Journal of the Acoustical Society of America*, Vol. 46, No. 6, 1969, pp. 1391–1396.

[12]Crocker, M. J., Cohen, R., and Wang, J. S., "Recent Development in the Design of Turbulent Microphone Windscreens for In-Duct Fan Sound Power Measurements," *Proceedings of Inter-Noise 73 Conference* (Copenhagen, Denmark), Inst. of Noise Control Engineering, New York, 1973, pp. 594–598.

[13]Wang, J. S., and Crocker, M. J., "Tubular Windscreen Design for Microphones for In-Duct Fan Sound Power Measurements," *Journal of the Acoustical Society of America*, Vol. 55, No. 3, 1974, pp. 568–575.

[14]Neise, W., "Theoretical and Experimental Investigation of Microphone Probes for In-Duct Fan Sound Power Measurements," *Journal of Sound and Vibration*, Vol. 39, No. 3, 1974, pp. 371–400

[15]Shepherd, I. C., and LaFontaine, R. F., "Microphone Screens for Acoustic Measurements in Turbulent Flows," *Journal of Sound and Vibration*, Vol. 111, No. 1, 1986, pp. 153–165.

[16]Anon., *Condenser Microphones and Microphone Preamplifiers for Acoustic Measurements: Data Handbook*, Brüel and Kjaer, Copenhagen, Denmark, 1982.

[17]Blake, W. K., "Turbulent Boundary-Layer Wall-Pressure Fluctuations on Smooth and Rough Walls," *Journal of Fluid Mechanics*, Vol. 44, Pt. 4, 1970, pp. 637–660.

[18]Bendat, J. S., and Piersol, A. G., *Random Data: Analysis and Measurement Procedures*, 2nd ed., Wiley, New York, 1986, pp. 137 and 285.

[19]Willmarth, W. W., "Pressure Fluctuations Beneath Turbulent Boundary Layers," *Annual Review of Fluid Mechanics*, Vol. 7, 1975, pp. 13–38.

[20]Kovasznay, L. S. C., "Hot Wire Method," *Physical Measurements in Gas Dynamics and Combustion*, Vol. 9, Art. F2, Princeton Univ. Press, Princeton, NJ, 1954, pp. 219–276.